Nuclear Materials and Energy xxx (xxxx) xxx–xxx

Contents lists available at ScienceDirect

Nuclear Materials and Energy

journal homepage: www.elsevier.com/locate/nme

He ion implantation induced He bubbles and hardness in tungsten

Cui Minghuan[a,*], Shen Tielong[a,*], Pang Lilong[a], Zhu Yabin[a], Jin Peng[a,b], Liu Chao[a,b], Fang Xuesong[a,b], Wang Zhiguang[a]

[a] *Institute of Modern Physics, CAS, Lanzhou 730000, China*
[b] *University of Chinese Academy of Sciences, Beijing 100049, China*

A B S T R A C T

The pure tungsten was implanted with 500 keV helium (He) ions to a fluence of 1.0×10^{17} ions/cm^2 at RT and 800 °C. After the implantation, cross-sectional transmission electron microscope (TEM) and nano-indentation measurements were used to investigate the He bubbles and hardness profiles induced by He implantation. Visible He bubbles were observed only in the damage peak region at RT but in the whole damage region at 800 °C. The size of He bubbles at 800 °C increased with increasing depths. With increasing the implantation temperature from RT to 800 °C, the size of He bubbles in the damage peak regions increased. The nano-indentation tests indicated that hardening was induced by He implantation at RT and 800 °C. The implantation induced peak hardness values were the same at both temperatures, but the hardness peaks moved to the surface with increasing temperatures. The formation of He bubbles and the contributions of their distribution and sizes to the hardness were discussed.

1. Introduction

Tungsten is a potential candidate divertor material in fusion reactors, due to its high melting point, high thermal conductivity, low activation, low sputtering and low hydrogen (H) isotope retention etc. [1]. Under operations, the divertor i.e. tungsten, will suffer from the irradiation of intense neutrons, the bombardments of helium (He) and H plasmas, and high heat fluxes. Therefore, He atoms could be introduced into tungsten by the He plasma bombardments and the (n, α) reactions under neutron irradiation. The microstructure, surface morphology and physical property changes of tungsten materials induced by He are important issues because they relate to the safe operation of the reactors. There were many researches focusing on these problems by using He ion implantation, which was an effective way to introduce He in materials because of its advantages such as short time, low cost, low activation. A large number of experimental results about the surface modification of tungsten after the implantation of He with high fluxes, high fluences and low energies (few ten to hundred eV), were reported [1–3]. They showed that He implantation induced surface morphology to change, such as the formation of tungsten fuzzes, holes and nanometric bubble layers, which closely related to He bubbles. Nano-indentation technology (NIT) is a useful tool to characterize the implantation induced hardening in micrometer regions and has been used in many studies on ion irradiation induced hardening [4–12]. The He induced hardness changes of tungsten were studied with NIT [6,8–10,12]. The relationships between He induced defects and mechanical properties were investigated based on the positron annihilation data [9,10], which could not give an intuitionistic evidence of He induced defects. The He induced defects in tungsten could be observed with transmission electron microscope (TEM) technology, which had been widely used in ion irradiation materials. Recently, the He bubbles in tungsten was observed with TEM and the effects of them to hardness increase were investigated as a function of He implantation fluence [12]. In addition to the fluence, the temperature also plays an important role in He bubble evolutions. Therefore, the motivation of our work is to give the direct evidence of He bubbles in tungsten, and to investigate the effects of He bubble distribution to hardness profiles at different temperatures. In this work, pure tungsten samples were implanted with 500 keV He ions at room temperature (RT) and 800 °C to produce a damaged layer containing He bubbles. The cross-sectional TEM observation was carried out to acquire the distribution and sizes of implantation induced He bubbles. The NIT was used to obtain the implantation induced hardness change.

2. Experimental details

The investigated samples were cut from high-pur tungsten materials. The samples were firstly mechanically polished and then annealed in vacuum at 1000 °C for 13 hours to reduce the work hardening. After these treatments, the samples were implanted with 500 keV He ions at

* Corresponding authors.
E-mail addresses: mhcui@impcas.ac.cn (M. Cui), shentielong@impcas.ac.cn (T. Shen), zhgwang@impcas.ac.cn (Z. Wang).

https://doi.org/10.1016/j.nme.2018.05.004
Received 29 November 2017; Received in revised form 7 March 2018; Accepted 8 May 2018

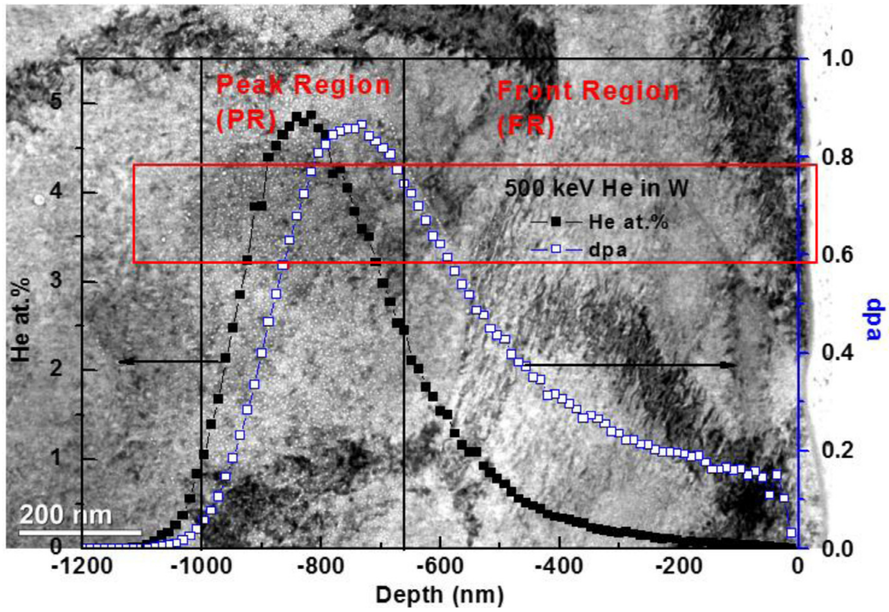

Fig. 1. TEM morphology in W induced by 500 keV He at 800 °C and corresponding dpa and He concentration profiles. (For interpretation of the references to color in the text, the reader is referred to the web version of this article.)

RT and 800 °C at the 320 kV Multi-Discipline Research Platform for Highly Charged Ions in Institute of Modern Physics, Chinese Academy of sciences (IMP, CAS), Lanzhou, China. The ion beams were swept in two perpendicular directions to a uniform distribution. The implantation fluence was 1.0×10^{17} ions/cm^2.

When the incident He ions irradiated into the samples, the major damages were the displacement damage (i.e. dpa, displacement per atom) and the He atom deposition. The theoretical results of dpa levels and He concentrations of the implanted samples were calculated with SRIM (The stopping and Range of Ions in Matter), and shown in Fig. 1. The displacement energy of tungsten (W) was set to be 90 eV [13]. As recommended in Ref. [14], both the surface energy and binding energy were set to be 0 eV, meanwhile we selected the mode of "Ion Distribution and Quick Calculation of Damage". It can be seen from Fig. 1 that the depths of peak dpa and the peak He atom concentration are about 740 and 830 nm from surface, respectively. The peak dpa and He concentration are about 0.86 dpa and 4.8 at. %, respectively. The He concentration in the first 200 nm is about 0.06 at. %. We define the region from surface to about 650 nm as the front region (FR) and define the region from 650 nm to 1000 nm as the peak region (PR), which are shown in Fig. 1.

After implantation, the implantation induced He bubbles were observed with cross-sectional TEM samples, which were prepared by using a FIB device. The TEM observation was performed in a FEI-TF20 operating at 200 kV. He bubbles were observed under different foci but only the images under focus were given in this work. In addition, NIT tests were carried out using an Agilent Nano Indenter G200 with a Berkovich tip (20 nm in radius) in the continuous stiffness mode (CSM). The indenter was normal to the sample's surface. Six indentations were carried out in each sample. Each indentation was set to be 2 um in depths and 30 um apart in order to avoid any overlap of the deformation region caused by other indentations.

3. Results and discussions

Low magnification TEM image of the tungsten sample implanted at 800 °C is shown in Fig. 1. The corresponding profiles of the dpa and He concentration are also given in the figure. It shows that the He implantation induces large amount of He bubbles, especially in the 650–1000 nm (the PR region), which is consistent with the calculated peak He concentration region. In addition to the He bubbles in the PR region, there are also many dense but small He bubbles in the FR region of the sample implanted at 800 °C. Fig. 2 shows the larger magnification TEM images of the red frame region shown in Fig. 1. In the first 50 nm under the surface, there is no He bubbles observed which may be the result of He desorption at the high temperature. From about 50 nm to 1000 nm, there are many He bubbles and the size of He bubbles becomes larger with increasing depths which is similar with the observation in Chines Low Activation Martensite (CLAM) steels implanted with He [15].

For the sample implanted at RT, He bubbles were observed only in the PR region and no bubbles were observed in the FR region probably because their sizes were smaller than the resolution of TEM. Fig. 3 gives the typical TEM images in the PR regions of samples implanted with He at RT and 800 °C. The sizes of He bubbles in the PR region at RT are similar with those in the FR region of sample at 800 °C, though the He concentration in the first 200 nm is about 1/80 of that in the peak. It means the critical He content of visible He bubble formation at 800 °C is less than 1/80 of that at RT, which is similar with the work reported by Iwakiri [16]. The average diameter and number density in the PR region at 800 °C are 3.81 ± 0.77 nm and 2.39×10^{17} /cm^3, respectively. The size of bubbles in the PR regions grows larger with increasing temperature from RT to 800 °C, though their He concentration are the same. Vacancies were not thermally mobile and He bubbles grew through ejecting interstitials at RT. While at 800 °C, He bubbles could grow by absorption of mobile vacancies including irradiation induced vacancies and thermal vacancies. Therefore the implantation induced bubbles are larger at 800 °C than at RT.

Previous studies showed that bubbles were strong obstacles that acted as barriers to dislocation motion, resulting in the increase of hardness of irradiated materials [4,11,12]. Therefore, we analyze the nano-hardness of samples to infer the contribution of He bubble's size and distribution to the mechanical properties of tungsten. Fig. 4(a) shows the average nano-hardness of the six indentations as a function of indentation depths for implanted samples and the un-implanted sample. Due to the uncertainty of indenter geometry and testing artifacts, hardness data between the surface and 50 nm are not reliable. Thus, we take the values at the depth deeper than 50 nm for analysis. For the implanted samples, hardness values are all larger than those of the un-implanted sample, which indicates ion implantation induces hardening